Medicine®

OPEN

Clinical application of high-resolution MRI in combination with digital subtraction angiography in the diagnosis of vertebrobasilar artery dissecting aneurysm

An observational study (STROBE compliant)

Meng Zhang, MD[a], Gengfan Ye, MD[b], Yuandong Liu, MD[c], Qian Wang, MD[d], Shuying Li, MD[e], Yunyan Wang, MD[b,*]

Abstract

Vertebrobasilar artery dissecting aneurysm (VBA-DA) is associated with serious complications and poor prognosis in patients. High-resolution magnetic resonance imaging (HR-MRI) is a noninvasive method for the diagnosis of VBA-DA.

VBA-DAs were classified according to the feature of HR-MRI in combination with digital subtraction angiography (DSA), and the clinical outcomes of different types of VBA-DAs were analyzed. Thirty-nine patients with 42 VBA-DAs were included and underwent HR-MRI, including three-dimensional T1 weighted image, three-dimensional T2 weighted image (3D-T2WI), three-dimensional time of flight MRA (3D-TOF-MRA), and three-dimensional fast imaging employing steady state acquisition (3D-FIESTA), and hematoma and flaps were compared. The follow-up was 3 to 25 months. The VBA-DAs were classified based on the images of HR-MRI and DSA, and the prognosis was analyzed.

VBA-DAs more frequently occurred on the vertebral artery, especially on the dominant vertebral artery. 3D-TOF-MRA showed high signal from hematoma, and 3D-FIESTA showed high signal from flaps. Based on HR-MRI images in combination with DSA, VBA-DAs were classified into 4 types: classical, stenosis, spiral, and hemorrhagic. The patients with the classical VBA-DAs had a higher improvement rate and a lower exacerbation rate. The patients with spiral and hemorrhagic VBA-DAs had poor clinical outcomes. The patients with stenosis VBA-DAs had poorer clinical outcomes than classical types and better clinical outcomes than spiral and hemorrhagic types.

The detection of intramural hematoma and dissection flap using HR-MRI provides basic information for the diagnosis of VBA-DA. Individualized therapeutic strategies can be designed for the treatment of VBA-DAs with different features of DSA and HR-MRI.

Abbreviations: 3D-FIESTA = three-dimensional fast imaging employing steady state acquisition, 3D-T1WI = three-dimensional T1 weighted image, 3D-T2WI = three-dimensional T2 weighted image, 3D-TOF-MRA = three-dimensional time of flight MRA, CTA = computed tomography angiography, DIR = double inversion recovery, DSA = digital subtraction angiography, HR-MRI = high-resolution magnetic resonance imaging, MRA = magnetic resonance angiography, mRS = modified Rankin Scale, QIR = quadruple inversion recovery, SAH = subarachnoid hemorrhage, TCD = transcranial cerebral Doppler, TE = echo time, TR = repetition time, VBA-DA = Vertebrobasilar artery dissecting aneurysm.

Keywords: aneurysm, dissection, high resolution, magnetic resonance imaging, vertebrobasilar artery

1. Introduction

Vertebrobasilar artery dissecting aneurysm (VBA-DA) is a pathological condition of the vertebrobasilar artery caused by hypertension, atherosclerosis, alpha-antitrypsin deficiency, neoplasm, trauma, infection, and/or inflammation.[1,2] Hematoma between intima and media can progressively occlude the parent artery, thus leading to decreased perfusion of the distal perforator vessels and even cerebral infarction. Even worse, ruptured VBA-DAs can lead to subarachnoid hemorrhage (SAH),

[a] Department of Neurosurgery, Hospital of Shandong Traditional Chinese Medicine University, [b] Department of Neurosurgery, QiLu Hospital, Shandong University, Jinan, [c] Department of Neurosurgery, Penglai Municipal People's Hospital, Penglai, [d] Department of Radiology, [e] Department of Radiotherpay, QiLu Hospital, Shandong University, Jinan, Shandong Province, People's Republic of China.

* Correspondence: Yunyan Wang, Department of Neurosurgery, QiLu Hospital, Shandong University, Jinan 250012, Shandong Province, People's Republic of China (e-mail: wangyunyan0618@yeah.net).

and eventually death of the patients.[3] The incidence rate of VBA-DA is approximately 1/100,000 to 1.5/100,000.[4] Young patients with VBA-DA often have ischemic symptoms, whereas old patients have bad prognosis due to hemorrhage.[5,6] Therefore, it is important to identify potential methods for the detection of VBA-DAs.

Conventionally, digital subtraction angiography (DSA), which is regarded as the "gold standard" method for the diagnosis of cerebrovascular disease, is also widely used for the diagnosis of VBA-DA.[7] Computed tomography angiography (CTA), magnetic resonance angiography (MRA), and transcranial cerebral Doppler have also been widely used for the diagnosis of VBA-DAs too. The primary feature of VBA-DA is intramural hematoma in the real and false lumen. Although traditional techniques such as DSA can differentiate inflow from outflow via dynamic blood flow, they can only display the morphology of the blood vessel not the structure of the vascular wall and the dissection flap. Identifying the location of intramural hematoma and the dissection flap is important for treating VBS-DAs correctly. High-resolution magnetic resonance imaging (HR-MRI) is the only noninvasive method for imaging the structure of vascular wall.[8] The scanning sequences of HR-MRI include three-dimensional T1 weighted image (3D-T1WI), three-dimensional T2 weighted image, three-dimensional time of flight MRA (3D-TOF-MRA), and three-dimensional fast imaging employing steady state acquisition (3D-FIESTA). These methods are noninvasive and repeatable, and exhibit high resolution to the dissection structure, such as intramural hematoma and flap.[9–12]

This study aimed to characterize the features of VBA-DA in 39 patients (with 42 VBA-DAs) including dissection size, morphology, and location. In addition, this study proposed a new clinical classification for VBA-DAs based on HR-MRI in combination with DSA, and analyzed the prognosis associated with each type of VBA-DAs. This classification provides the clinical basis for individualized treatment of different VBA-DAs.

2. Methods

2.1. Study design and patient population

The study was approved by the Medical Ethics Committee of QiLu Hospital, Shandong University, and all patients gave their written informed consent. From November 2013 to October 2015 44 patients were recruited with suspected VBA-DAs and visited the Department of Neurosurgery of QiLu Hospital, Shandong University. The following patients were included in the present study: had suspected VBA-DA detected by DSA; had the aneurysms involved in the vertebral artery, basilar artery, and/or vertebrobasilar artery; and underwent HR-MRI examination. The following patients were excluded from the present study: had dissecting aneurysms involved in nonvertebrobasilar artery regions; had nondissecting aneurysms with calcification or atherosclerosis confirmed by CT or MRI; uncooperative; had SAH with Hunt–Hess grade IV; and no MRI examination.

2.2. High-resolution magnetic resonance imaging

All patients underwent HR-MRI scanning with a 3.0T GE device (HDx 3.0 T, GE Healthcare, Chicago, IL). MRI scans were performed in 8 channel head and neck coils with a matrix size of 256×256 pixels and a pixel size of $0.28\,mm \times 0.28\,mm$. The lesion region was identified by 3D-TOF-MRA. Lesions in the vascular wall such as intramural hematoma, atherosclerosis,

calcification, and false and true lumen were identified using the black blood and white blood techniques. The black blood techniques employed quadruple inversion recovery (QIR) and 3D-T1WI non-double inversion recovery and traditional T1WI. QIR eliminated blood flow artifact to a larger extent, and improved spatial resolution. 3D-T1WI had high contrast signal intensity on T1-weighted image, which was superior on the diagnosis of lesions on the vascular wall. 3D-FIESTA was adopted in the white blood technique to reveal fine dissection structure, such as flap. The MR sequences parameter were as follows: 3D-TOF-MRA, repetition time (TR), 22 millisecond; echo time (TE), 3.2 millisecond; field of view (FOV), 240×240 mm^2. 3D-T1WI: TR, 8.6 millisecond; TE, 3.4; FOV, 240×240 mm^2. 3D-FIESTA: TR, 4.7 millisecond, TE, 1.5 millisecond; and FOV, 240×240 mm^2.

2.3. Imaging analysis

Two experienced neuroradiologists independently reviewed the images on post-processing workstation in a double-blind way. The final diagnosis was made by discussion and approved among neuroradiologists, neurointerventionists, and neurologists. If there was conflicted diagnosis, the final diagnosis would be made by an experienced cerebrovascular neurologist. Image quality was classified as follows: grade 1 for excellent, uniform images with no apparent flow artifacts; grade 2 for good images with only minor flow artifacts; and grade 3 for the images not suitable for analysis. The images of grade 1 and 2 were included in the present diagnosis.

2.4. Follow-up

All patients were followed up for 3 to 25 months by telephone. Among the 39 patients, 30 patients underwent DSA during the follow-up. Prognosis were scored on the basis of modified Rankin Scale (mRS) score,[13] as follows: mRS ≤ 1, improvement; $2 \leq mRS \leq 3$, stabilization; and mRS ≥ 4, exacerbation.

2.5. Statistical analysis

Statistical analyses were performed using SPSS version 19.0 (International Business Machines Corporation (IBM), Armonk, New York). Quantitative data are expressed as mean ± standard deviation. Categorical data were expressed as the percentage. Differences were analyzed using Fisher's exact test. $P < .05$ was considered statistically significant.

3. Results

3.1. Baseline characteristics of patients

Of the 44 patients who were initially enrolled, 5 patients were excluded, including 2 SAH patients with Hunt–Hess grade IV, 1 patient with extensive calcification of basilar artery diagnosed by HR-MRI and CTA, and 2 patients with atherosclerosis confirmed by CT and MRI. Finally, 39 patients with 42 dissecting aneurysms were included in the study. Three patients had bilateral aneurysms. All 39 patients with VBA-DA underwent stent-assisted coiling embolization after preoperative examination.

The mean age of the patients was 57.69 ± 8.66 years (range, 42–72 years, Table 1). Of the 39 patients, 28 patients were male and 11 patients were female. Twenty-one patients (53.8%) had hypertension, and 8 patients (20.5%) had diabetes. Twelve patients smoked cigarettes. Headache or neck pain was the most

Table 1

The baseline characteristics of patients.

	Patients (n = 39)
Number of aneurysm (n)	42
Age (year, mean, range)	57.69 ± 8.66
Male	28 (71.8%)
Female	11 (28.2%)
Hypertension	21 (53.8%)
Diabetes	8 (20.5%)
Smoking	12 (30.8%)
Clinical presentation	
Headache or neck pain	17 (43.6%)
Inarticulate speech or limb numbness	9 (23.1%)
Dizziness	13 (33.3%)
Cerebellar signs	5 (12.8%)
Imaging presentation	
Stroke on DWI	7 (17.9%)
SAH on CT	6 (15.4%)

CT = computed tomography, DWI = diffusion weighted imaging, SAH = subarachnoid hemorrhage.

clinical manifestation, followed by dizziness, inarticulate speech or limb numbness, and cerebellar signs. Seven patients had stroke confirmed by DWI and 6 patients had SAH diagnosed by CT.

3.2. Dissection location

Table 2 showed the location of the 42 VBA-DAs, and Figure 1 showed the representative images. VBA-DAs more frequently occurred in the vertebral artery (30/42, 71.4%), and less frequently occurred in the basilar artery (8/42, 19.1%) and the left vertebrobasilar artery (4/42, 9.5%). Aneurysms were more frequently located proximally to the posterior inferior cerebellar artery (PICA) than distally to the PICA and in the PICA (66.7% [28/42], 11.9% [5/42], and 21.4% [9/42] respectively). Of the 42 aneurysms, 19 (45.2%) aneurysms occurred at the ventrolateral region and 23 (45.2%) aneurysms occurred at the dorsolateral region of the artery. Of the 39 patients, 21 (53.8%) patients had

Table 2

Location of aneurysms.

Characteristics	n
Involved vascular DA	42
Left vertebral artery	16 (38.1%)
Right vertebral artery	14 (33.3%)
Basilar artery	8 (19.1%)
Left vertebrobasilar artery	4 (9.5%)
Right vertebrobasilar artery	–
Relationship with PICA	42
Proximal to PICA	5 (11.9%)
In PICA	9 (21.4%)
Distal to PICA	28 (66.7%)
Location of dissection	42
Ventral-ventrolateral region	19 (45.2%)
Dorsal-dorsolateral region	23 (54.8%)
Vertebral artery dominance	21 (53.8%)
Left vertebral artery	17 (81.0%)
Right vertebral artery	4 (19.0%)
VBA-DA in vertebral artery dominance or not	21
Vertebral artery dominance	20 (95.2%)
Non-vertebral artery dominance	1 (4.8%)

"–" = not evaluated, DA = dissection aneurysm, PICA = posterior inferior cerebellar artery, VBA-DA = vertebrobasilar artery dissecting aneurysm.

vertebral artery dominance and 18 (46.2%) patients had no vertebral artery dominance. In 21 patients with vertebral artery dominance, the left side of the dominance was found in 17 patients (81.0%). VBA-DAs more often occurred on the dominant vertebral artery (20/21, 95.2%) than on the nondominant vertebral artery (1/21, 4.8%).

3.3. Detection of hematoma and flap by HR-MRI scanning sequences

Figure 2 showed the representative images of VBA-DA on HR-MRI. The hematoma and flaps detected by 3D-TOF-MRA, 3D-T1WI, and 3D-FIESTA, were compared (Table 3). 3D-TOF-MRA showed the signal of hematoma and flap was 57.1% (24/42) and 52.4% (22/42), 3D-T1WI showed 23.8% (10/42) and 9.5% (4/42), and 3D-FIESTA showed 47.6% (20/42) and 61.9% (26/42), respectively. 3D-TOF-MRA had the highest signal of hematoma, and 3D-FIESTA has the higher signal of flap (Table 3).

3.4. Detection of atherosclerotic plaque by HR-MRI scanning sequences

HR-MRI clearly detected the difference between VBA-DAs and atherosclerotic plaques in the vascular wall. For atherosclerotic lesions, the incrassated intima was eccentric and inhomogeneous on HR-MRI images, whereas the dissection always exhibited homogenous signals on HR-MRI images (Fig. 3). More importantly, atherosclerotic plaque was enhanced in enhancement scan, and did not occur in VBA-DAs.

3.5. Clinical classification of VBA-DA

Based on HR-MRI and DSA images (Fig. 4), VBA-DAs were classified into 4 types: classical, stenosis, spiral, and hemorrhagic, which occurred in 19 cases (48.7%), 6 cases (15.4%), 8 cases (20.5%), and 6 cases (15.4%) of the 42 aneurysms, respectively.

3.6. Clinical prognosis

All 39 patients were followed up for 3 to 25 months, with a median follow-up period of 13 months. Of the 39 patients, 30 (76.9%) patients underwent DSA during follow-up. The prognosis was significantly difference among patients with different types of VBA-DAs (chi-squared test = 8.917, P = .015; Table 4). The patients with classical VBA-DAs had a high improvement rate and a lower exacerbation rate compared with the spiral type (P = .032), and hemorrhagic type (P = .048) (Table 4). The patients with spiral and hemorrhagic VBA-DAs had poor clinical outcomes. The patients with stenosis VBA-DAs had poorer clinical outcomes than classical types and better clinical outcomes than spiral and hemorrhagic types.

4. Discussion

Although the development of surgical instruments and therapeutic methods greatly improves the treatment of VBA-DA, the prognosis of patients with VBA-DA is still poor.[14] In addition, the clinical outcomes of patients with VBA-DA are largely depended on the location and dissection structure.

VBA-DAs were more frequently found on the vertebral artery than on the basilar artery, suggesting that anatomic factors of posterior circulation may contribute to the formation of VBA-DAs.
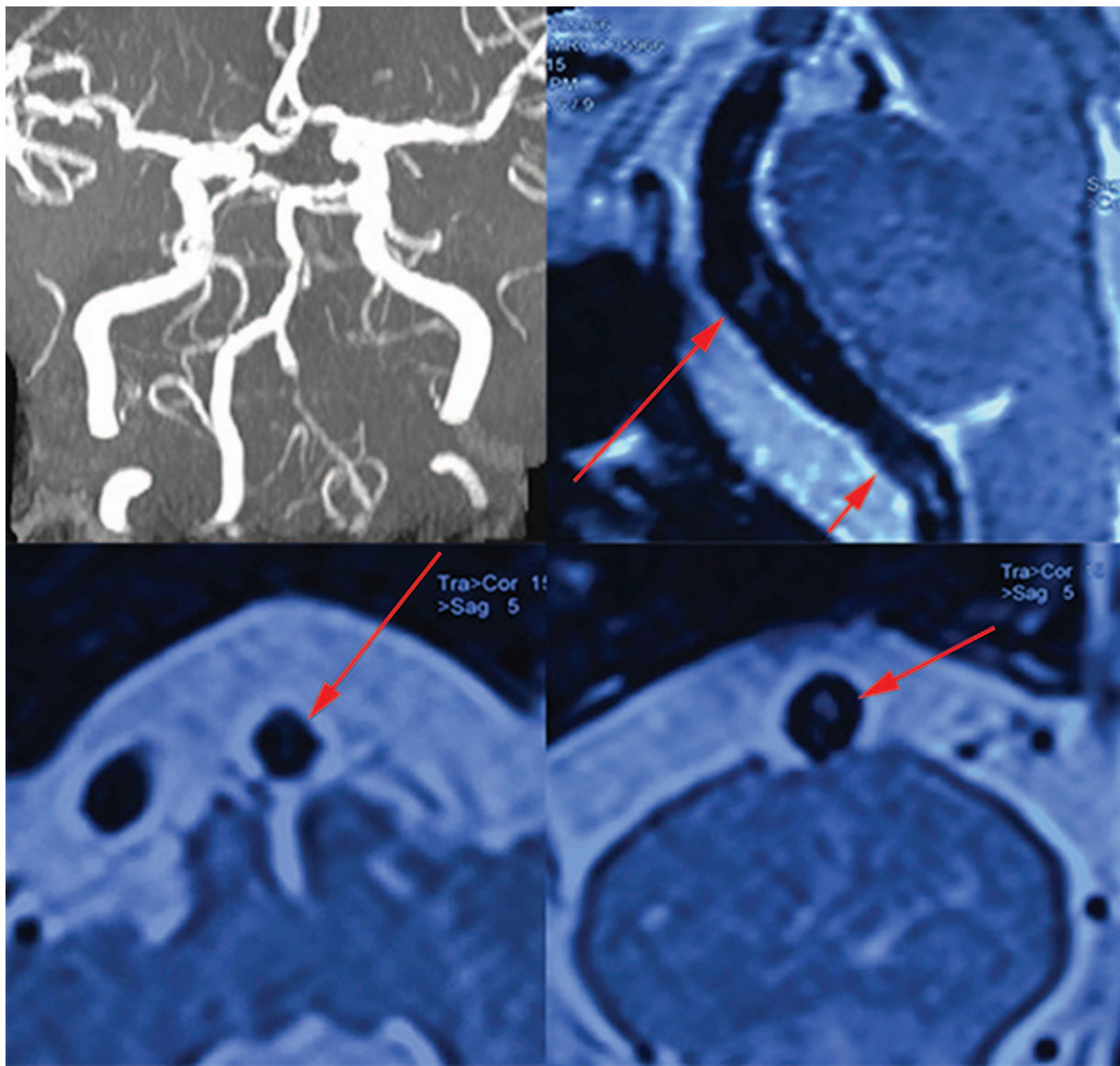
Figure 1. 3D-DSA and HR-MRI images of VBA-DAs on different locations. a1 and a2, 3D-DSA images show the VBA-DAs that involve the vertebral artery with 2 dissecting aneurysms proximal and distal to the PICA in the dominant VA (a1), and a dissecting aneurysm in the PICA in the non-dominant VA (a2). b1 and b2: 3D-DSA images show the dissecting aneurysm in the basilar artery, but not in the vertebral artery. c1 and c2: 3D-DSA images show that a dissecting aneurysm involves both the vertebral artery and basilar artery. d1 and d2: HR-MRI images show that VBA-DAs with intramural hematoma are located in the ventrolateral region (d1) and dorsolateral region (d2). The white arrows indicate intramural hematoma. DSA = digital subtraction angiography, HR-MRI = high-resolution magnetic resonance imaging, PICA = posterior inferior cerebellar artery, VBA-DA = vertebrobasilar artery dissecting aneurysm.

The vertebral artery has less connective tissues and is vulnerable to head movement, and thus may be susceptible to vascular damage and occurrence of VBA-DA. Approximately 50% of patients had vertebral artery dominance, which is consistent with the previous report by Hong et al.[15] In addition, VBA-DAs more frequently occurred on the dominant vertebral artery than on the nondominant vertebral artery, suggesting that hemodynamics factors contribute to the formation of VBA-DAs. The high blood flow in the dominant vertebral artery can increase the pressure on internal wall. The fluid shear stress can produce "crimping effect" on the vascular wall and long-term crimping effect will result in damage to the intima, eventually leading to the formation of VBA-DAs.

HR-MRI can clearly show the vascular wall and lumen structure with the black blood and white blood techniques. Blood flow presents to be black and the vessel wall exhibits high signal intensity in the black blood technique. White blood technique can clearly visualize the wall structure and obtain high spatial resolution images by enhancing the contrast between blood flow and vessel wall.[8,12,16–18] The presence of intramural hematoma and dissection flap in the HR-MRI is important for diagnosing VBA-DA. In this study, 3D-TOF-MRA and 3D-FIESTA were sensitive for detecting intramural hematoma and dissection flap. Although 3D-T1WI was less sensitive, the contrast and resolution of images, especially the outline of dissection flap, were good enough for diagnosis of VBA-DA.

Although DSA is widely used for diagnosis of VBA-DA, it is associated with many disadvantages: an invasive procedure with a risk for blood vessel damage; unsuitable for frequent studies; and cannot show the structure of the vascular wall and dissection flap. In contrast, HR-MRI is a useful noninvasive tool for
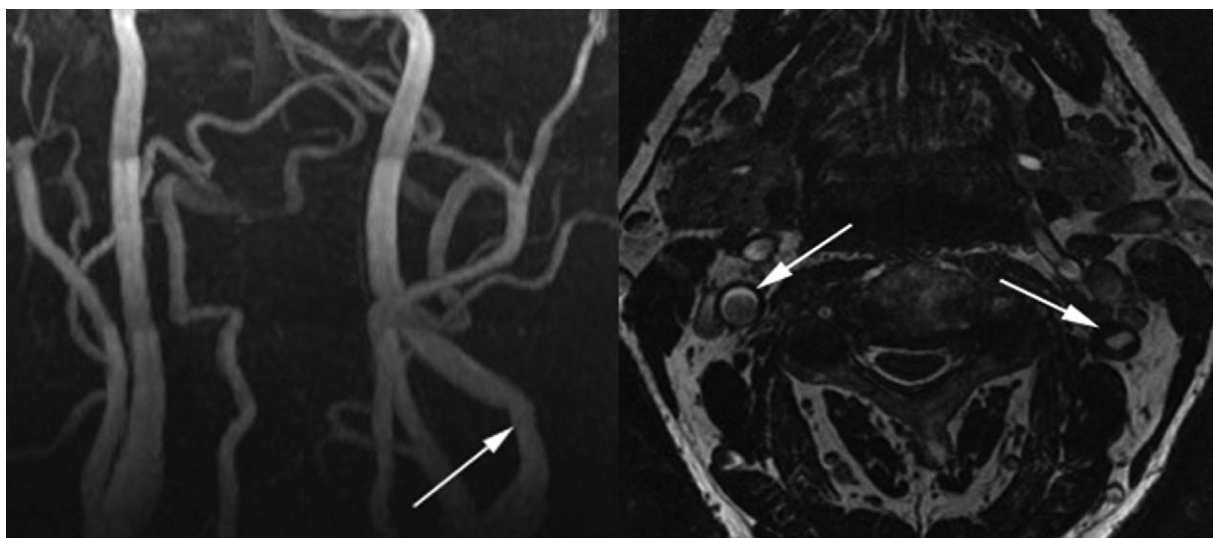
Figure 2. Representative images of VBA-DA on HR-MRI. A and D: DSA images; B: 3D-TOF-MRA image; C and F: 3D-FIESTA images; E: 3D-T1WI image. Arrow "a" indicates the true lumen; arrow "b" indicates the false lumen, representing dissection or crescent intramural hematoma. An abnormal signal line between "a" and "b" indicates the flap. 3D FIESTA = three-dimensional fast imaging employing steady state acquisition, 3D-T1WI = three-dimensional T1 = weighted image, 3D-TOF-MRA = three-dimensional time of flight magnetic resonance angiography, HR-MRI = high-resolution magnetic resonance imaging, VBA-DA = vertebrobasilar artery dissecting aneurysm.

diagnosis of VBA-DA. HR-MRI can visualize the vascular wall structure. 3D-TOF-MRA has a high signal from hematoma and 3D-FIESTA has a high signal from flap. In addition, HR-MRI has a great contrast and high spatial resolution, which can improve diagnostic accuracy. In addition, since HR-MRI is noninvasive and feasible for the diagnosis of VBA-DA.

Traditionally, VBA-DA are classified into ischemic and hemorrhagic types.[19] In this study, we proposed a new classification of VBA-DA based on the HR-MRI images in combination with DSA images. According to the dissection morphology and perforating branches, VBA-DAs are classified into 4 types: classical, stenosis, spiral, and hemorrhagic type (Fig. 3). In the classical type, the dissection was characterized by expansion of vascular disease without rupture. Hematoma is primarily located between the media and adventitia. In the stenosis type, hematoma was mainly located between the intima and media. Stenosis occurred in the proximal or distal end of the dissecting aneurysms and involved some perforating branches, eventually leading to ischemic stroke. In the spiral type, the dissection exhibited dolichoectasia in DSA. Interestingly, spiral variation on different segment could be revealed clearly from the axial images on HR-MRI (Fig. 3C1). In the hemorrhagic type, the

dissection was comparable to that in the classical type. In this type, the adventitia was ruptured and the blood flows into the subarachnoid space. The internal structure of VBA-DAs on HR-MRI provided useful information for clinical diagnosis.

In addition, we examined the prognosis of patients with different types of VBA-DAs. We found that patients with the classical type of VBA-DAs were associated with good clinical outcome, possible because this type of VBA-DAs only caused vascular dilatation without the involvement of perforating branches. In contrast, patients with the spiral and hemorrhagic types were associated with poor outcomes. In the spiral type, the internal elastic lamina was severely damaged due to the fluid shear stress or the crimping effect on the intima. The perforating branches could be involved to cause stenosis or occlusion. Moreover, microthrombus from the inner-dissection resulted in acute ischemic stroke. The worse prognosis of patients with the spiral type of VBA-DA may be associated with stenosis or occlusion of the vessels and even the presence of acute ischemic stroke. The worse prognosis of patients with the hemorrhagic type of VBA-DA may be associated with SAH, which can induce serious cerebrovascular vasospasm, and cause severe acute ischemic stroke, hydrocephalus, or obstructive hydrocephalus.

For the stenosis type, the therapeutic strategies were determined by the local conditions of the stenosis. If the stenosis was caused by intramural hematoma or thrombosis, single stent-assisted coils embolization should be sufficient for the purse of protecting some involved perforating branches. Winspan stent or Enterprise stent with strong support are preferred to use. Prior to implant the stents, Gateway balloon is advised to use to dilate the blood vessel. If the stenosis is caused by atherosclerosis, the narrow vessel should be dilated with the balloon before single stent-assisted coils embolization. For the spiral type, multiple stent-assisted coils embolization should be applied to get better therapeutic effects. To avoid stent moving during coil introduction, the first stent should be deployed with stent semi-deploying technique or stent post-deploying technique. Since perforating branches are involved in this type, loosened coil embolization

Table 3

Scanning sequences and findings on HR-MRI.

	Hematoma	Flap
3D-TOF-MRA	24 (57.1%)*	22 (52.4%)†
3D-T1WI	10 (23.8%)	4 (9.5%)
3D-FIESTA	20 (47.6%)‡	26 (61.9%)§

3D FIESTA = three-dimensional fast imaging employing steady state acquisition, 3D-T1WI = three-dimensional T1 = weighted image, 3D-TOF-MRA = three-dimensional time of flight magnetic resonance angiography, HR-MRI = high-resolution magnetic resonance imaging.

* $P < .01$ 3D-TOF-MRA vs. 3D-T1WI (chi-squared test = 10.22).
† $P < .01$ 3D-TOF-MRA vs. 3D-T1WI (chi-squared test = 18.69).
‡ $P < .05$ 3D-FIESTA vs. 3D-T1WI (chi-squared test = 5.42).
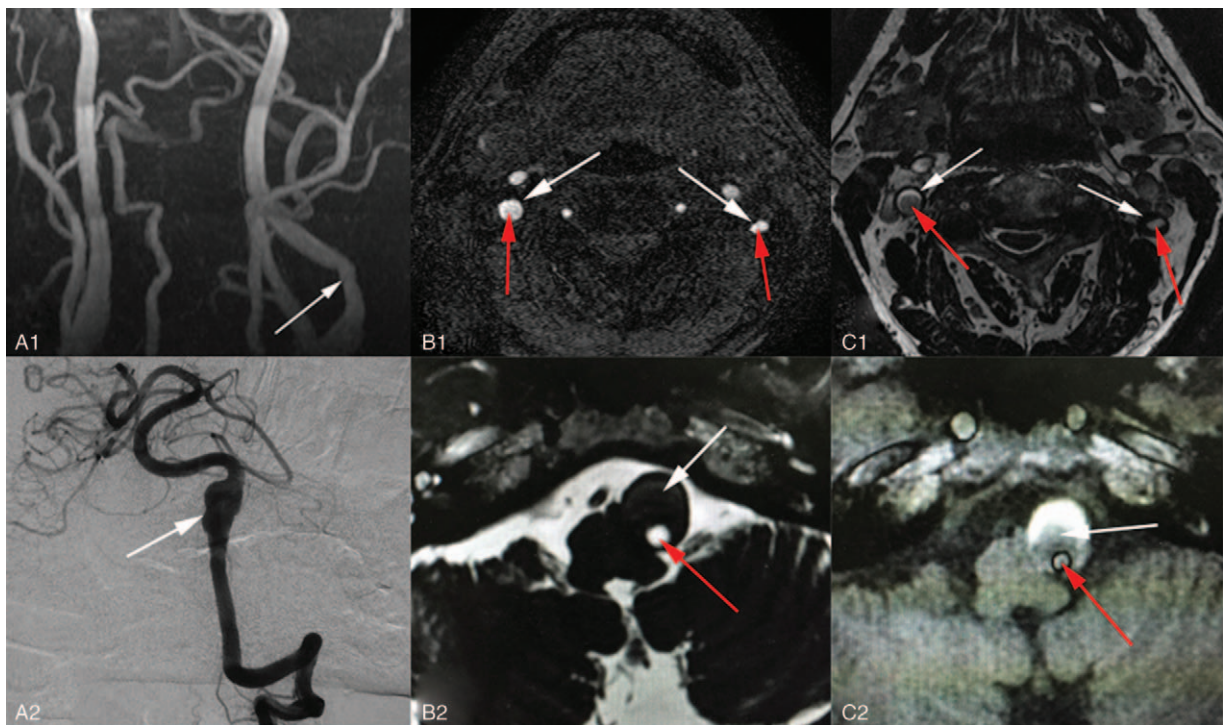§ $P < .01$ 3D-FIESTA vs. 3D-T1WI (chi-squared test = 26.22).

Figure 3. HR-MRI can distinguish dissecting aneurysms from atherosclerotic lesions. A1, B1, and C1 show atherosclerotic lesions on DSA (A1), 3D-TOF-MRA (B1), and 3D-FIESTA (C1) images. Red arrows indicate vascular cavity; left white arrows indicate thickened intima of the blood vessel; right white arrows indicate normal intima of the blood vessel. A2, B2, and C2 show VBA-DAs on DSA (A2), 3D-TOF-MRA (B2), and 3D-FIESTA (C2) images. Red arrows indicated intramural hematoma; white arrows indicate vascular cavity. 3D FIESTA = three-dimensional fast imaging employing steady state acquisition, 3D-TOF-MRA = three-dimensional time of flight magnetic resonance angiography, DSA = digital subtraction angiography, HR-MRI = high-resolution magnetic resonance imaging, VBA-DA = vertebrobasilar artery dissecting aneurysm.
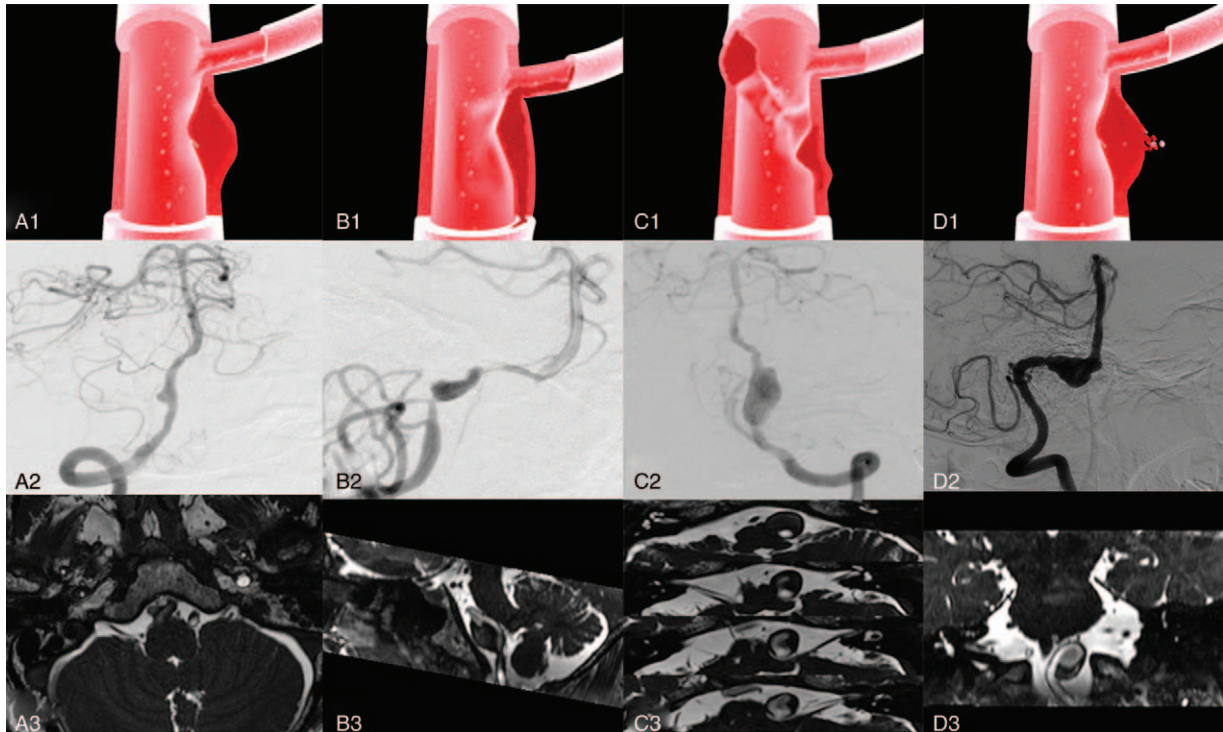

Figure 4. Four classification of VBA-DA based on DSA and HR-MRI. A1, B1, C1, and D1 represent classical type, stenosis type, spiral type, and hemorrhagic type, respectively. A2, B2, C2, and D2 show DSA images of VBA-DA and A3, B3, C3, and D3 show HR-MRI images. An arrow in A1 shows the intramural hematoma. A crescent signal out of vessel lumen in A3 image indicates intramural hematoma. In the B3 image, vascular stenosis is proximal to the hematoma. In the C3 images, the position of hematoma varies with the changes of vessel segment, indicating the spiral type. D1–D3 images represent ruptured dissecting aneurysms with SAH (cranial CT not display). In the D2 image, the morphology of aneurysm is anomalous. The intramural hematoma and flap are displayed clearly in the D3 image. A layer crossing the arterial lumen indicates a dissection flap. DSA = digital subtraction angiography, HR-MRI = high-resolution magnetic resonance imaging, SAH = subarachnoid hemorrhage, VBA-DA = vertebrobasilar artery dissecting aneurysm.

Table 4

Clinical outcome of patients with different types of VBA-DAs.

Groups	Improvement	Stabilization	Exacerbation	IR	ER
Classical type	16	3	0	84.2%	0.0%
Stenosis type	3	3	0	50.0%	0.0%
Spiral type	2	4	2	25.0%	25.0%[*]
Hemorrhagic type	3	1	2	50.0%	33.3%[†]

Differences in IR and ER among the 4 groups were analyzed using Fisher's exact test (*P* = .015). Pairwise comparison.

IR = improvement rate, ER = exacerbation rate, VBA-DA = vertebrobasilar artery dissecting aneurysm.

[*] *P* = .032, classical type vs. spiral type.

[†] *P* = .048, classical type vs. hemorrhagic type.

should be used to protect the perforating branches and decrease postoperative complications. For the hemorrhagic type, to reduce re-bleeding risk of ruptured dissection, multiple stent-assisted technique and compact coils embolization should be considered to be the first choice. To avoid aneurysmal rupture due to extrusion of the implanted coils, stent should be deployed completely following coils embolization through the mesh of stent.

This study has some limitations: pathological specimen and histopathology examination were not performed because it was dangerous to collect the sample of the vertebrobasilar artery. Therefore, the diagnostic symptoms including intramural hematoma and dissection flap were only determined by imaging and clinical experience, and the final diagnosis is not confirmed by pathohistological examination. This study only included 42 VBA-DAs in 39 patients. The sample size was relative small. Future study with a large sample size will be performed to confirm our findings in the present study.

In summary, we studied the clinical features of 42 VBA-DAs in 39 patients. We compared the effect of different HR-MRI sequences on detection of hematoma and flap, and found that 3D-TOF-MRA and 3D-FIESTA exhibited greater sensitivity and thus were useful for diagnosis of VBA-DA. Moreover, a new classification of VBA-DA was provided. Based on our classification, individualized therapeutic strategies can be designed for the treatment of VBA-DA.

Author contributions

Conceptualization: Yunyan Wang.
Data curation: Meng Zhang, Gengfan Ye, Qian Wang, Shuying Li, Yunyan Wang.
Formal analysis: Meng Zhang, Gengfan Ye, Yuandong Liu, Qian Wang, Yunyan Wang.
Methodology: Meng Zhang, Yuandong Liu, Yunyan Wang.
Supervision: Yunyan Wang.
Validation: Gengfan Ye, Shuying Li.
Writing – original draft: Meng Zhang, Gengfan Ye, Yunyan Wang.
Writing – review & editing: Meng Zhang, Gengfan Ye, Yuandong Liu, Qian Wang, Shuying Li, Yunyan Wang.

References

[1] Santos-Franco JA, Zenteno M, Lee A. Dissecting aneurysms of the vertebrobasilar system. A comprehensive review on natural history and treatment options. Neurosurg Rev 2008;31:131–40.

[2] Yoon WK, Kim YW, Kim SR, et al. Angiographic and clinical outcomes of stent-alone treatment for spontaneous vertebrobasilar dissecting aneurysm. Acta Neurochir (Wien) 2010;152:1477–86.

[3] Ro A, Kageyama N. Pathomorphometry of ruptured intracranial vertebral arterial dissection: adventitial rupture, dilated lesion, intimal tear, and medial defect. J Neurosurg 2013;119:221–7.

[4] Kobayashi N, Murayama Y, Yuki I, et al. Natural course of dissecting vertebrobasilar artery aneurysms without stroke. AJNR Am J Neuroradiol 2014;35:1371–5.

[5] Ruecker M, Furtner M, Knoflach M, et al. Basilar artery dissection: series of 12 consecutive cases and review of the literature. Cerebrovasc Dis 2010;30:267–76.

[6] Gottesman RF, Sharma P, Robinson KA, et al. Imaging characteristics of symptomatic vertebral artery dissection: a systematic review. Neurologist 2012;18:255–60.

[7] Cai J, Wu D, Mo Y, et al. Comparison of extracranial artery stenosis and cerebral blood flow, assessed by quantitative magnetic resonance, using digital subtraction angiography as the reference standard. Medicine (Baltimore) 2016;95:e5370.

[8] Chung JW, Kim BJ, Choi BS, et al. High-resolution magnetic resonance imaging reveals hidden etiologies of symptomatic vertebral arterial lesions. J Stroke Cerebrovasc Dis 2014;23:293–302.

[9] Naggara O, Louillet F, Touze E, et al. Added value of high-resolution MR imaging in the diagnosis of vertebral artery dissection. AJNR Am J Neuroradiol 2010;31:1707–12.

[10] Shi MC, Wang SC, Zhou HW, et al. Compensatory remodeling in symptomatic middle cerebral artery atherosclerotic stenosis: a high-resolution MRI and microemboli monitoring study. Neurol Res 2012; 34:153–8.

[11] Han M, Rim NJ, Lee JS, et al. Feasibility of high-resolution MR imaging for the diagnosis of intracranial vertebrobasilar artery dissection. Eur Radiol 2014;24:3017–24.

[12] Ryu CW, Kwak HS, Jahng GH, et al. High-resolution MRI of intracranial atherosclerotic disease. Neurointervention 2014;9:9–20.

[13] Puri AS, Massari F, Asai T, et al. Safety, efficacy, and short-term follow-up of the use of Pipeline Embolization Device in small (<2.5 mm) cerebral vessels for aneurysm treatment: single institution experience. Neuroradiology 2016;58:267–75.

[14] Chen L, Xu L, Yang D, et al. The management of vertebrobasilar dissecting aneurysm using endovascular embolization. Cell Biochem Biophys 2014;70:149–55.

[15] Hong JM, Chung CS, Bang OY, et al. Vertebral artery dominance contributes to basilar artery curvature and peri-vertebrobasilar junctional infarcts. J Neurol Neurosurg Psychiatry 2009;80: 1087–92.

[16] Oppenheim C, Touze E, Leclerc X, et al. High resolution MRI of carotid atherosclerosis: looking beyond the arterial lumen. J Radiol 2008;89(3 Pt 1):293–301.

[17] Xu WH, Li ML, Niu JW, et al. Luminal thrombosis in middle cerebral artery occlusions: a high-resolution MRI study. Ann Transl Med 2014;2:75.

[18] Jia ZJ, Zhao R, Yang ZG, et al. Intracranial atherosclerotic middle cerebral arterial stenosis research based on 3.0 Tesla high-resolution magnetic resonance imaging: recent progress. Nan Fang Yi Ke Da Xue Xue Bao 2015;35:154–9.

[19] Park KW, Park JS, Hwang SC, et al. Vertebral artery dissection: natural history, clinical features and therapeutic considerations. J Korean Neurosurg Soc 2008;44:109–15.